

Electrostatic interactions and staging in graphite intercalation compounds

S. A. Safran and D. R. Hamann

Bell Laboratories, Murray Hill, New Jersey 07974

(Received 25 February 1980)

The nonlinear Thomas-Fermi equations which describe the screening of intercalant layers in graphite intercalation compounds are solved analytically in the approximation that the graphite *c*-axis band dispersion is neglected. The total energy of the system of charged intercalant layers and the self-consistent charge distribution are calculated analytically for *general* configurations of the intercalant layers. Because of electrostatic screening, *pure stage* configurations minimize the total (electrostatic plus band) energy for fixed chemical potential. Estimates of the stage dependence of both the electrostatic and elastic interactions between intercalant layers are presented. Experimental tests of these mechanisms for staging are suggested.

Graphite intercalation compounds are characterized by an ordered sequence of n carbon and one intercalant layer with n defining the stage of the material.^{1,2} A wide variety of chemical and physical differences are associated with the different stage compounds. The explanation of the existence of pure stage materials as the equilibrium products of the intercalation process in graphite^{3,4} can be pursued on three levels: (i) the classes of interactions which give rise to pure stages [Fig. 1(a)]—in contrast to those interactions which result in more complicated one-dimensionally modulated structures [e.g., Fig. 1(b)], (ii) the microscopic origins of the interactions responsible for staging, and (iii) the effects of finite temperature on both the stage and the in-plane intercalant concentration. A previous paper⁵ presented a discussion of (i) and (iii) in a calculation of the phase diagram for staged intercalation compounds which used a phenomenological model for the intercalant interactions. In this work, we address (i) and (ii) and use a self-consistent, nonlinear, Thomas-Fermi approximation⁶ to calculate analytically the electrostatic repulsive interaction energy between intercalant layers that have donated their charges to the graphite host. The electrostatic interaction energies are compared with estimates of the elastic interaction energies between intercalants in graphite intercalation compounds,^{7,8} since both are possible sources of stage ordering. We show that electrostatic screening implies that the lowest energy state of graphite intercalation compounds (at fixed chemical potential) is given by pure stage ordering. Although elastic interactions are important in the *kinetics* of intercalation and staging, the electrostatic interactions dominate in *equilibrium* for completely intercalated materials where the repulsive coherency strains vanish.^{7,8}

The screening of the intercalant layers by the charges donated to the graphite is a problem of current interest. In particular, the magnetic sus-

ceptibility of graphite intercalation compounds has been shown to be particularly sensitive to the *c*-axis charge distribution.⁹⁻¹¹ In Sec. I, we summarize the Thomas-Fermi equations for the self-consistent charge distribution in graphite intercalation compounds. This formulation was first suggested by Pietronero *et al.*⁶ who calculated the *c*-axis charge distribution using a numerical integration of the Thomas-Fermi equations. For the case of a single intercalant layer in an infinite graphite medium, they showed that the screening of the intercalant follows a power law with a potential $\phi(z)$ of the form $\phi(z) \sim (z + z_0)^{-2}$. The nonexponential nature of the screening is associated with the (approximately) zero density of states at the Fermi level for unintercalated material. In Sec. II, we derive an *analytic* expression for the total (band plus electrostatic) energy in the approximation that the *c*-axis graphite band dispersion is neglected. In contrast to the numerical results of Ref. 6, our expressions are valid for any general configuration of intercalant layers. We thus show how the long-range, screened electrostatic interactions imply the existence of pure stage ordering in contrast to the more complicated structures generally found in systems with long-range binary interactions.⁵ Section III presents a calculation of the energies of pure stage materials, including estimates of the magnitude and stage dependence of both electrostatic and elastic interactions. The theory is compared with experiment^{3,4} and suggestions for further experiments are presented in Sec. IV.

I. SUMMARY OF THOMAS-FERMI EQUATIONS

In this section, we derive the Thomas-Fermi equations which describe the *c*-axis charge distribution in graphite intercalation compounds. As in Ref. 6, we assume that the charge is homogeneously distributed in the layers perpendicular to the *c*-axis. Since stage ordering exists in graphite in-

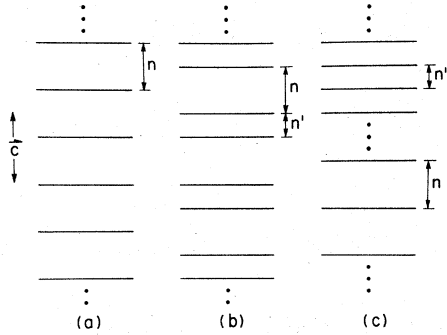


FIG. 1. Possible c -axis orderings of the intercalate layers in graphite intercalation compounds (Ref. 5) (only the intercalate layers are shown). (a) Pure stage ordering: a periodic sequence of an intercalate layer, n graphite layers, (b) Nonpure stage ordering: a periodic sequence of intercalate layers more complicated than that of (a). Shown here is a sequence of intercalant, n graphite, intercalant, n' graphite, (c) Mixed phase: a macroscopic mixture of pure stages n and n' .

tercalation compounds with a wide variety of in-plane orderings¹² (commensurate or incommensurate with host) or disorder¹³ (lattice-gas, liquidlike) the details of the in-plane intercalant ordering do not seem to be crucial. Furthermore, one can show that corrections to our theory due to the in-plane intercalant structure consist of exponentially small terms of the form e^{-Gz} , where G is the smallest intercalant layer reciprocal-lattice vector. These terms can be neglected in comparison with the *power law* interactions obtained here. In addition to assuming a homogeneous charge distribution perpendicular to the c axis, we use a continuum approximation to represent the nonhomogeneous charge distribution between the intercalant layers. Since our interest lies in the interaction between intercalant layers, the neglect of the discrete nature of the graphite layers should be a good approximation for high stages where the distance between intercalant layers is much larger than the 3.35 Å which separate adjacent graphite layers. Along with the neglect of the discrete nature of the graphite layers, we neglect the effects of the small c -axis band dispersion of the graphite energy bands.

Since we are interested in the interaction energy of the intercalant layers, we derive the Thomas-Fermi equations describing the charge distribution from an energy density formalism¹⁴ where the electrostatic and band energy is written in a Hartree approximation as

$$E(n) = \frac{1}{2} \int [V_1(z) - V_2(z)][n(z) - \rho(z)] dz + \int \epsilon_b(n(z))n(z) dz. \quad (1)$$

In Eq. (1) $n(z)$ and $\rho(z)$ are the carrier and ion charge distributions, respectively—the charge is assumed to be homogeneously distributed perpendicular to the c axis. $\epsilon_b(n)$ is the total band energy per electron due to in-plane graphite band dispersion only. The first term in Eq. (1) is the electrostatic energy and $V_1(z)$ and $V_2(z)$ satisfy

$$\frac{\partial^2 V_i(z)}{\partial z^2} = -\frac{4\pi e^2}{\epsilon} \theta_i(z), \quad i=1,2 \quad (2)$$

where $\theta_1 = n(z)$ and $\theta_2 = \rho(z)$. In Eq. (2), ϵ is the graphite c -axis dielectric constant^{15,16} which accounts for the screening of the intercalant ions due to the bonding π electrons and σ electrons which are not explicitly considered in this calculation.

For small shifts of the Fermi level of the two-dimensional (single-layer) graphite band structure,¹⁰

$$\epsilon_b(n) = \frac{2}{3} \beta n^{1/2}, \quad (3)$$

where for a single graphite layer with q intercalant atoms per carbon and a charge transfer of f electrons per intercalant,

$$\beta n^{1/2} = \gamma_0 (\pi 3^{1/2} q f)^{1/2}. \quad (4)$$

In Eq. (4) γ_0 is the tight-binding matrix element ($\gamma_0 \approx 3$ eV). Minimizing the energy [Eq. (1)] with respect to $n(z)$ and using Eqs. (2) and (3) one can write Poisson's equation for the total electrostatic potential $\phi(z)$ as

$$\frac{\partial^2 \phi}{\partial z^2} = \tau^2 [\bar{n}(z) - \bar{\rho}(z)]. \quad (5)$$

Here we have used dimensionless units for the charge distributions $\bar{n}(z)$ and $\bar{\rho}(z)$ with

$$\bar{n}(z) = n(z)c_0/\sigma, \quad (6)$$

$$\bar{\rho}(z) = \rho(z)c_0/\sigma. \quad (7)$$

In Eqs. (6) and (7) c_0 is the spacing between adjacent carbon planes ($c_0 = 3.35$ Å) while $\sigma = \sigma_c/6$ where σ_c is the planar density of carbon atoms. The potential ϕ is dimensionless and

$$\tau^2 = \frac{4\pi e^2 (\sigma/c_0)^{1/2}}{\epsilon \beta}$$

is related to the ratio of Coulomb to band energies. If ϵ_b and the potential ϕ have their zeros defined by the Fermi level of neutral graphite, we find that the minimization of Eq. (1) yields the nonlinear relationship between the potential and the charge density:

$$\phi^2(z) = \bar{n}(z). \quad (8)$$

We now introduce the dimensionless length $\xi \equiv z\tau$ and rewrite Eqs. (5) and (8) as

$$\frac{\partial^2 \phi}{\partial \xi^2} = \bar{n}(\xi) - \bar{\rho}(\xi), \quad (9a)$$

$$\phi^2(\xi) = \bar{n}(\xi). \quad (9b)$$

The intrinsic nonlinearity of these equations arises from the zero density of states at the Fermi level for a single graphite layer. For a finite density of states, ϕ and \bar{n} would be linearly related to lowest order. Using this notation, the energy per intercalant can be written

$$\bar{\epsilon} = \frac{q}{6N_0} \left(\frac{1}{2} \int \phi(\xi) \bar{\rho}(\xi) d\xi + \frac{1}{6} \int \phi^3(\xi) d\xi \right), \quad (10a)$$

$$\bar{\epsilon} = \frac{E\tau/c_0}{N\beta(\sigma/c_0)^{1/2}}, \quad (10b)$$

where N is the total number of intercalant atoms and N_0 is the number of intercalant layers.

To facilitate an analysis of the intercalant-intercalant interactions and orderings, we solve Eq. (9) for a general configuration of intercalant layers. A given configuration is characterized by cells labeled by j , of length c_j , with n_j graphite layers separated by intercalant layers with charges p_j (in the units described above) so that

$$\bar{\rho}(\xi) = \sum_j \delta(\xi - \xi_j) p_j.$$

Figure 2 illustrates the cell notation used in our calculations. Within each cell, i.e., for $\xi_j < \xi < \xi_{j+1}$,

$$\frac{\partial^2 \phi}{\partial \xi^2} = \phi^2 \quad (11)$$

with the boundary conditions

$$\phi(\xi_j^+) = \phi(\xi_j^-), \quad (12)$$

$$\phi'(\xi_j^+) - \phi'(\xi_j^-) = -p_j, \quad (13)$$

where the prime signifies differentiation with respect to ξ and where

$$\xi_j^\pm = \xi_j \pm |\eta|$$

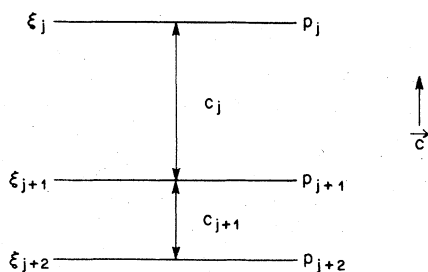


FIG. 2. Notation describing a general configuration of intercalant layers. The j th intercalant layer with charge p_j is located at ξ_j . Each pair of intercalant layers (j and $j+1$) defines a cell of length c_j .

as $\eta \rightarrow 0$. The first condition, Eq. (12), expresses the continuity of the potential across the intercalant sheets, while the second condition, Eq. (13), relates the jump in the electric field to the intercalant ion charge.

To solve the system of Eqs. (11)–(13) we multiply Eq. (11) by $2\phi'(\xi)$ and integrate to obtain

$$\phi'(\xi) = \pm (\frac{2}{3})^{1/2} (\phi^3 - \phi_{0,j}^3)^{1/2}, \quad (14)$$

where $\phi_{0,j} = \min[\phi(\xi)]$ in the interval $\xi_j < \xi < \xi_{j+1}$ so that $\phi_{0,j} = 0$ (see Fig. 3). Since we are interested in the dependence of the energy on the intercalant-intercalant separation, it is unnecessary to solve explicitly for ϕ as a function of ξ (see Sec. II). Instead, we parametrize the problem in terms of c_j , p_j , $\phi_{0,j}$, and ϕ_j where $\phi_j = \phi(\xi_j)$ as shown in Fig. 3. From Eqs. (12)–(14) we find

$$(\phi_j^3 - \phi_{0,j-1}^3)^{1/2} + (\phi_j^3 - \phi_{0,j}^3)^{1/2} = (\frac{3}{2})^{1/2} p_j. \quad (15)$$

The \pm sign in Eq. (14) has been chosen such that Eq. (13) is satisfied for $p_j > 0$. Integrating Eq. (14) from $\xi_j < \xi < \xi_{j+1}$ with signs appropriately chosen, we obtain ($c_j \equiv \xi_{j+1} - \xi_j$)

$$c_j = (\frac{3}{2})^{1/2} \left(\int_{\phi_{0,j}}^{\phi_j} g(\phi) d\phi + \int_{\phi_{0,j}}^{\phi_{j+1}} g(\phi) d\phi \right), \quad (16)$$

where

$$g(\phi) = (\phi^3 - \phi_{0,j}^3)^{-1/2}. \quad (17)$$

Thus, we find equations which, in general, couple the potential at the intercalant layer and the potential minimum to those of all the other cells. However, for pure stage configurations, Eqs. (15) and (16) are merely a pair of nonlinear coupled equations whose solutions are discussed in Sec. II. Here, we note that for general configurations of the intercalant layers, one can solve Eqs. (15)–(17) in the approximation that most of the transferred charge is localized near the intercalant layer

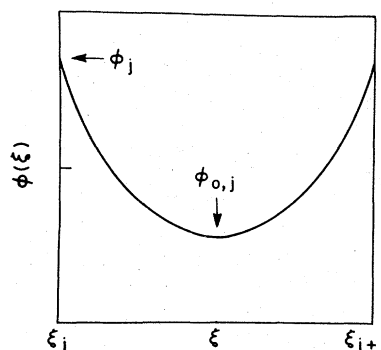


FIG. 3. Schematic plot of the electrostatic potential $\phi(\xi)$ as a function of distance ξ in a given cell (see Fig. 2). ϕ_j is the potential at the cell boundary while $\phi_{0,j}$ is given by $\phi_{0,j} = \min[\phi(\xi)]$ for $\xi_j < \xi < \xi_{j+1}$.

er so that $\phi_{0,j} \ll \phi_j$. One then finds

$$\phi_j \approx v_j \left(1 + \frac{\phi_{0,j}^3 + \phi_{0,j-1}^3}{6v_j^3} \right), \quad (18)$$

$$v_j = \left(\frac{q}{8} \right)^{1/3} p_j^{2/3}, \quad (19)$$

$$\phi_{0,j} \approx \sqrt{12} \pi^2 (c_j + d_j + d_{j+1})^{-2}. \quad (20)$$

In Eq. (20), the dimensionless, nonlinear "screening lengths" d_j and d_{j+1} are related to the charges on the j th and $(j+1)$ th intercalant layers, respectively, with

$$d_j = (24)^{1/3} p_j^{-1/3}. \quad (21)$$

The expressions in Eqs. (18)–(21) are exact to order r_j^3 where

$$r_j \equiv \phi_{0,j} / \phi_j \quad (22)$$

as given above. The order r_j^3 equations are sufficient for an evaluation of the energy to this order. The small parameter in the expansion is always r_j^3 so that the next term in the energy behaves as r_j^6 . Numerical estimates of ϕ_j and $\phi_{0,j}$ will be presented in Sec. III where the energetics of pure stages are discussed. Here we note that the lowest-order term for the minimum of the potential in the unit cell $\phi_{0,j}$ has the form expected from the application of the asymptotic form of the potential for a *single layer*⁸ given above.

II. ANALYTIC EXPRESSION FOR TOTAL ENERGY

In this section, we derive a formula for the total (band plus electrostatic) energy of graphite intercalation compounds using the model theory presented in Sec. I. We show that to a good approximation the lowest-energy configuration of a set of intercalant layers is a pure stage configuration [Fig. 1(a)] under conditions of fixed chemical potential if the electrostatic repulsive interaction is dominant.

In the Appendix we show that the energy per intercalant (in our units) can be written

$$\bar{\epsilon} = \frac{q}{90N_0} \left(9 \sum_j \phi_j p_j + \sum_j \phi_{0,j}^3 c_j \right). \quad (23)$$

This expression is exact within our Thomas-Fermi model. By using the approximations for ϕ_j and $\phi_{0,j}$ presented in Eqs. (18)–(20) we can find the energy to order r_j^3 . Equation (23) can then be rewritten

$$\bar{\epsilon} \approx \frac{q}{90N_0} \left(9 \left(\frac{q}{8} \right)^{1/3} \sum_j p_j^{5/3} + \sum_j \phi_{0,j}^3 (c_j + d_j + d_{j+1}) \right), \quad (24)$$

where $\phi_{0,j}$ is given by Eq. (20). The first sum in Eq. (24) is independent of the separation of the intercalant layers and is just the sum of the energies

of isolated layers in an infinite graphite medium. The second sum in Eq. (24) represents the self-consistently screened intercalant-intercalant repulsive interaction. Substituting Eq. (20) we find

$$\phi_{0,j}^3 (c_j + d_j + d_{j+1}) = (12)^{3/2} \pi^6 (c_j + d_j + d_{j+1})^{-5}.$$

The next term in the expression for $\bar{\epsilon}$ is of order $(c_j + d_j + d_{j+1})^{-11}$, since it arises from terms of order $r_j^6 (c_j + d_j + d_{j+1})$. These terms are thus negligible for large intercalant-intercalant separations.

For the case $p_j = p$, applicable to zero temperature where each intercalant layer is at its "close-packing" density, $d_j = d$ and we can write

$$\bar{\epsilon} \approx \epsilon_\infty(p) \left(1 + \frac{\alpha}{N_0} \sum_j (1 + \frac{1}{2} c_j/d)^{-5} \right), \quad (25)$$

where

$$\epsilon_\infty(p) = (3^{1/3} q/20) p^{5/3} \quad (26a)$$

and

$$\alpha = \pi^6 3^{1/2} / 1728 \approx 0.9636. \quad (26b)$$

The total energy is thus the sum of all the individual cell energies (each depending on c_j) but with no terms involving products such as $c_j c_{j+1}$ so that $\bar{\epsilon}$ is *independent* of the configuration of the cells within our approximations. Higher-order terms in our expansion would produce coupling between cells. For example, higher-order expansions of ϕ_j involve terms such as $\phi_{0,j} \phi_{0,j-1}$ which lead to products involving c_j and c_{j-1} . The effective interaction between layers described by Eq. (25) is unusual in the sense that one *cannot* consider a given layer (say at $\xi = 0$) as interacting with other layers according to some function $V(\xi)$ where $V(\xi)$ is a simple, continuous function. Instead, a given layer interacts with its nearest-neighbor layers through some function $V_a(\xi)$ and with its next-nearest neighbors through *another function* $V_b(\xi)$. In our case, we have demonstrated that $V_a(\xi) \sim (1 + \xi/\xi_0)^{-5}$ while $V_b(\xi)$ is of order $(1 + \xi/\xi_0)^{-11}$. The two-body layer interactions are thus nonadditive and only nearest-neighbor interactions need be considered. The energy is then approximated as the sum of "cell" energies. The physical origin of this independence upon configuration is the screening of the intercalant layers so that the energies of the configurations shown in Figs. 1(b) and 1(c) are approximately degenerate.

At fixed chemical potential (μ), the internal energy of the intercalant system has the form

$$U = -\mu N + \bar{E} N, \quad (27)$$

where \bar{E} is the electrostatic and band energy per

intercalant and N is the total number of intercalants. In a continuum model for the graphite host (whose total volume is fixed) for a given value of μ , U is minimized by a lattice of intercalant layers with equal spacing, due to the repulsive interactions [Eq. (25)]. The lattice spacing is a continuous function of μ in this case. However, if one now constrains the separation of any two intercalant layers to be (within a constant) an integral number of graphite layer spacings, only pure stage configurations will have the same energies as those of the continuum limit. In our approximation, any microscopic configuration of intercalant layers with a total concentration in between that of two pure stages is degenerate with that of a macroscopic mixture of the two pure stage phases in appropriate proportions. Such configurations will necessarily have internal energies higher than those of the equally spaced lattice for the same concentration continuum model. Thus, the minimum on a curve of U as a function of N (for fixed μ) is always attained for the pure stages.

III. ELECTROSTATIC AND ELASTIC ENERGIES

In Sec. II, we derived an expression for the total (electrostatic plus band) energy based on a self-consistent solution of the nonlinear Thomas-Fermi equations. We showed that the minimum-energy configuration is given by a pure stage. In this section, we evaluate the energy for the pure stages and discuss the contribution of elastic interactions to stage ordering.

A. Electrostatic plus band energy

From Eqs. (25) and (26) one can write the energy for graphite intercalation compounds with stoichiometry $C_{12n}X$ (e.g., stage $n \geq 2$ alkali metals K, Rb Cs) as

$$\bar{E}(n) \approx E_\infty \{1 + \alpha [1 + x(n)]^{-5}\}. \quad (28)$$

In Eq. (28), $\bar{E} = E/N$ is the energy per intercalant. For unit charge transfer ($f=1$) $E_\infty \approx 1.1$ eV, $\alpha \approx 0.96$, and $x(n) \approx n/4.1$. For comparison with Ref. 6 we have used a value for the c -axis dielectric constant^{15,16} of $\epsilon \approx 5.4$. Figure 4 shows $\Delta E(n) \equiv \bar{E}(n) - E_\infty$ plotted as a function of concentration or inverse stage for both Eq. (28) (with n treated as a continuous variable) and a numerical solution of the nonlinear Thomas-Fermi equations for a staged configuration. Note that the stage dependence of the energy is not approximately n^{-5} for the stages of interest ($1 < n \leq 15$)—but is rather slower since the asymptotic form of $[1 + x(n)]^{-5}$ is not reached with 10% accuracy till $n \approx 200$. The energy is a monotonically decreasing function of stage, representing a repulsive interaction between nearest-

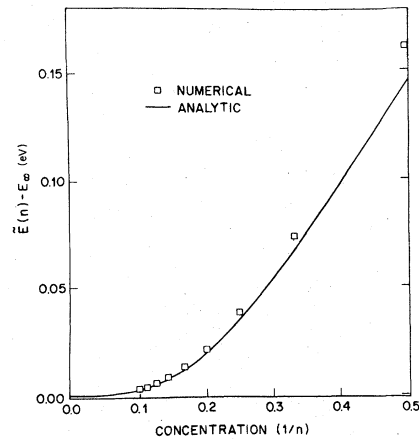


FIG. 4. Stage dependence of the total electrostatic and band energies as a function of intercalant concentration. The squares are the results of a numerical solution of the nonlinear Thomas-Fermi equations for stages $n = 2, \dots, 10$. The solid line is the analytical result calculated from Eq. (28) for a simple periodic sequence of intercalant layers with lattice spacing c_0/x , where x is the ratio of intercalant layers to carbon layers and $c_0 = 3.35$ Å.

neighbor intercalant layers.

B. Elastic interactions

An alternative origin for the repulsive interaction between intercalate layers that gives rise to staging is the elastic strain induced by the intercalate atoms due to the separation of the graphite layers. In previous publications^{7,8} we have shown that the elastic interaction between intercalants is long ranged. For a staged configuration of intercalant islands in an *infinite* graphite medium, the elastic interaction is repulsive and results in an energy per intercalant of $\Delta U_{\text{elas}} \approx 0.5$ eV/n. However, in a sample that is fully loaded with an array of intercalant stacks, these coherency strains vanish.^{7,8} Thus, for *fully intercalated* graphite single crystals in true equilibrium, one does not expect the long-range repulsive elastic energies to dominate the staging energetics. (See, however, Sec. IV for a discussion of the experiments.) Furthermore, since the elastic interaction is *not screened* there is no simple way to understand the existence of pure stage ordering as opposed to more complicated ordered sequences of intercalant layers. On the other hand, the electrostatic mechanism discussed above provides an explanation for pure stage ordering.

In addition to the repulsive elastic interaction due to the separation of graphite layers, there exists a small *attractive* elastic interaction between intercalants due to the change in the in-plane lattice constant of the graphite upon intercalation. As-

suming the intercalant atoms exert *in-plane* forces tending to contract or expand the (in-plane) lattice constant of the bounding graphite layers only (i.e., those layers of graphite that are adjacent to intercalant layers), one can write a phenomenological expression for the energy of this elastic distortion. For a compound with stoichiometry $C_{an}X$,

$$\Delta U_{\text{in-plane}} = q(n\bar{C}\epsilon^2 + 2\Delta_0\epsilon). \quad (29)$$

In Eq. (29) $\bar{C} \approx 68$ eV while the strain $\epsilon \equiv \Delta a/a$, where a is the graphite in-plane lattice constant.¹⁷ Δ_0 is the force on each bounding graphite layer. The factor of n appears in Eq. (29) since we have assumed that all n graphite layers in the unit cell between the intercalant layers maintain the same in-plane lattice constant. It is assumed that the energy of the misfit dislocations which would arise if the layers had different in-plane lattice constants is greater than the strain energies for these small (<1%) in-plane distortions. (Misfit dislocations are allowed for graphite layers separated by an intercalant layer.)

One immediately sees from Eq. (29) that the energy is minimized for

$$\epsilon = \epsilon_0/n,$$

where $\epsilon_0 = \bar{C}/\Delta_0$. This expression for ϵ is in agreement with experiments¹⁸ in $C_{12n}K$ which indicate $\epsilon_0 \approx 0.008$. Thus, the energy due to this in-plane strain $\Delta U_{\text{in-plane}} \approx -0.05$ eV/ n . This energy is lowest for stage 1 and hence can be termed an "anti-staging," attractive interaction between intercalant layers.¹⁹ Although this treatment neglects any coupling of the in-plane and c -axis strains, it does indicate that there is a long-range ($1/n$ dependent) attractive interaction, which at some stage must overcome the repulsive electrostatic interactions responsible for stage ordering. The competition of these energies thus results in some maximum possible stage. However, since the *precise* quantitative nature of the various energies involved is as yet unknown, numerical estimates of this effect are premature at this time.

IV. COMPARISON OF THEORY WITH EXPERIMENT

In this section we compare the theoretical discussion of Secs. I–III with experiment. Suggestions for further experiments are presented and we summarize the main theoretical results.

At low temperatures, where the intercalant layers are fully saturated, the intercalant configuration is a pure stage (see Sec. III) and is determined by the minimization of the internal energy [Eq. (27)]. In general, the energy per intercalant \bar{E}

$= E_0 + E_1(n)$, where only E_1 is a function of stage. One can then show that the range of chemical potential μ over which a given stage is stable $[\Delta\mu(n)]$ is given by⁵

$$\Delta\mu(n) = n[|E_1(n+1) + E_1(n-1) - 2E_1(n)|]. \quad (30)$$

Thus, measurements of the low-temperature range of stability of a given stage (determined by *in situ* structural measurements of both the stage and in-plane density) yield direct information about the interactions responsible for stage ordering. For example, for the electrostatic interactions discussed here [Eq. (28)], $E_1(n) \sim (1+n/n_0)^{-5}$, while for the elastic repulsive interaction (applicable only to crystals that are not fully intercalated), $E_1 \sim n^{-1}$.

Although no *in situ* structural and chemical potential (e.g., vapor pressure) experiments have as yet been reported, the "equilibrium" vapor pressure as a function of weight uptake has been measured for both alkali⁴ and iron chloride⁵ graphite intercalation compounds. A preliminary analysis of the alkali data seemed to *indicate*⁴ that the repulsive stage-dependent energy $E_1(n) \sim 0.5$ eV/ n , although the stage was only inferred from weight-uptake measurements and no high-stage ($n > 5$) data were reported. The need for precise, equilibrium, *in situ* studies of high-stage compounds is clear. One could speculate and relate the repulsive energy deduced from the early data of Ref. 4 to the repulsive interactions between intercalant layers due to the distortion of the surrounding *infinite* graphite matrix. This would imply that the samples were not fully intercalated or that grain boundary effects simulated the behavior of an infinite medium through clamping. Elastic clamping should play an important role in the kinetics of intercalation and might dominate if staging were a kinetic and not an equilibrium phenomenon.

On the other hand, for true equilibrium properties of *fully* intercalated crystals, the dominant repulsive intercalant-intercalant interaction should be the electrostatic repulsion which is long-ranged due to the nonexponential screening. We have solved the nonlinear Thomas-Fermi equations for the electrostatic potential and have self-consistently calculated the total (electrostatic plus band) energy for a general configuration of intercalant layers in the approximation that the graphite c -axis dispersion is neglected. Due to screening, the interaction is effective between a given intercalant layer and its first-neighboring intercalant layer (wherever it may be) and leads to pure stage ordering. Corrections to the simple, analytically tractable theory presented here due to c -axis dispersion effects are currently being pursued.²⁰

ACKNOWLEDGMENT

The authors thank P. C. Hohenberg for useful discussions.

APPENDIX

In this appendix, we present the steps leading from Eq. (10) to Eq. (23) for the total energy in our approximations. The first integral of Eq. (11) yields [Eq. (14)]

$$[\phi'(\xi)]^2 = \frac{2}{3}(\phi^3 - \phi_{0,j}^3). \quad (\text{A1})$$

Using this expression for ϕ^3 in Eq. (10) we find

$$\bar{\epsilon} = \frac{q}{6N_0} \sum_j \left[\frac{1}{2} \phi_j p_j + \frac{1}{6} \left(\frac{3}{2} \int' (\phi')^2 d\xi + \phi_{0,j}^3 \int' d\xi \right) \right]. \quad (\text{A2})$$

In Eq. (A2) the prime on the integral signifies integration over the j th cell only. The first integral in Eq. (A2) can be converted to an integral over the variable ϕ and has the form

$$\int' (\phi^3 - \phi_{0,j}^3)^{1/2} d\phi.$$

Rationalizing the numerator of this expression and integrating by parts, using Eq. (13) for the boundary conditions, results in Eq. (23).

¹J. E. Fischer and T. E. Thompson, *Phys. Today* **31** (7), 36 (1977).

²Proceedings of the International Conference on Layered Materials and Intercalates (Nijmegen, Netherlands, 1979) [*Physica (Utrecht)* **99B** (1980)].

³W. Metz and D. Hohlwein, *Carbon* **13**, 87 (1975).

⁴F. J. Salzano and S. Aronson, *J. Chem. Phys.* **44**, 4320 (1965).

⁵S. A. Safran, *Phys. Rev. Lett.* **44**, 937 (1980).

⁶L. Pietronero, S. Strässler, H. R. Zeller, and M. J. Rice, *Phys. Rev. Lett.* **41**, 763 (1978); *Solid State Commun.* **30**, 399 (1979).

⁷S. A. Safran and D. R. Hamann, *Phys. Rev. Lett.* **42**, 1410 (1979).

⁸S. A. Safran and D. R. Hamann, *Physica (Utrecht)* **99B**, 469 (1980).

⁹S. A. Safran, F. J. DiSalvo, R. C. Haddon, J. V. Waszczak, and J. E. Fischer, *Physica (Utrecht)* **99B**, 494 (1980).

¹⁰S. A. Safran and F. J. DiSalvo, *Phys. Rev. B* **20**, 4889 (1980).

¹¹F. J. DiSalvo, S. A. Safran, R. C. Haddon, J. V. Waszczak, and J. E. Fischer, *Phys. Rev. B* **20**, 4883 (1980).

¹²N. Kambe, M. S. Dresselhaus, G. Dresselhaus, S. Basu, A. R. McGhie, and J. E. Fischer, *Mater. Sci. Eng.* **40**, 1 (1979).

¹³H. Zabel, Y. M. Jan, S. C. Moss, *Physica (Utrecht)* **99B**, 463 (1980); R. Clarke, N. Caswell, S. A. Solin, and P. M. Horn, *Physica (Utrecht)* **99B**, 457 (1980).

¹⁴P. C. Hohenberg and W. Kohn, *Phys. Rev. B* **136**, 864 (1964).

¹⁵H. Venghaus, *Phys. Status Solidi* **81**, 221 (1977); M. Zanini, D. Grubisic, and J. E. Fischer, *Phys. Status Solidi B* **90**, 151 (1978).

¹⁶The actual c -axis dielectric constant for a small number of graphite layers depends on details of the c -axis hopping and is hence unknown.

¹⁷D. L. Blakslee, D. G. Proctor, E. J. Seldin, G. B. Spence, and T. Weng, *J. Appl. Phys.* **41**, 3373 (1970).

¹⁸D. E. Nixon and G. S. Parry, *J. Phys. C* **2**, 1732 (1969).

¹⁹This is in contrast to the conclusion of C. Kittel, *Solid State Commun.* **25**, 519 (1978).

²⁰S. A. Safran, in Proceedings of the Second International Conference on Intercalation Compounds of Graphite, Provincetown, Mass., 1980 [Synth. Met. (to be published)]; also, S. A. Safran and D. R. Hamann (unpublished).